The Effects of Nozzle Angle and Distance Between Burners on Burning Velocity in Counter Flames

Jassim M. Abdulkarim Jaff

Abstract— Premixed laminar combustion of liquefied petroleum gas (LPG) and air is studied experimentally using counterflowing axisymmetric jets. Attributes of this type of burner arrangement for studying laminar combustion are discussed in terms of flame geometry, angle of nozzle, burning velocities, and measurement access.

In the current research, an integrated combustion system was designed and developed for a type of counterflow premixed flame. To study formation of the double disc flame and the limits of stability, three types of nozzle with different angles (30°, 45°, and 60°) were used, and the shapes of this type of flame are blow-off flame, double flame, disc flame, and distortion flame. In order to get the disc of flame front stably and uniformly, an integrated design of two perpendicular burners was made to maintain the temperature of the mixture constant before the reaction.

Results are preliminary, a laminar burning velocity is observed and it appears to be related to the angle of nozzle burner.

Keywords— Counterflow, Premixed burner, Laminar Burning Velocity.

1 Introduction

Information of extinction limits of laminar flames under periodic strain is required to quantify the influence of length and time scales of flame quenching and to assist modeling of flame extinction.

In this context, unforced flame extinction has been examined theoretically, for example by [1] in laminar counterflow flames and [2] in turbulent counterflow flames, but forced flame extinction has received limited attention in spite of its importance to practical devices, such as gas turbine combustors, IC and air craft engines [3]. The optimization of practical combustion devices requires a detailed knowledge of the combustion kinetic.

Moreover, most practical combustion systems operate at pressures well above (0.1MPa) (gas turbines, aeronautic turbines, engines). The development and validation of detailed combustion mechanisms must therefore take into account the influence of temperature flame front. Most of the combustion kinetic mechanisms have been validated in nozzle (burner) laboratory conditions (flow, homogeneous reactors, and premixed flames) [4].

•*Dr. Jassim M. A. Jaff, lecturer in Department of Production Engineering, Sulaimani Polytechnic University, College of Technical Engineering-Sulaimani–Iraq.*
E-mail: dr.aljaaf@yahoo.com

1.1 Flame Geometry

Flames that exist in counterflowing axisymmetric streams are, in the mean, planar and circular, the flow is symmetric about the stagnation plane when the mass flow rates are the same from both nozzles, and the flow is independent of the angular coordinate.
This geometry approximates a one dimensional laminar flame subject to stretch. Combustion models for example on laminar flamelet crossing frequencies [5] or fractal properties of the flame surface [6] are well suited to the flat flames produced in counterflowing streams [7].

Premixed flames stabilized against an air or a fuel stream, and twin premixed flames of the same of air-fuel mixture compositions between the two streams. The premixed flames were characterized by equivalence ratio ϕL and ϕU of the fuel-air mixture in the lower and the upper tube, respectively, defined as [3].

$$\phi i = \left[\frac{(Q^{\cdot}fuel)i}{(Q^{\cdot}air)i}\right] * \left[\frac{(Q^{\cdot}fuel)st}{(Q^{\cdot}air)st}\right]^{-1} \quad (1)$$

Where ($Q^{\cdot}i$) is the metered volume flow rate of fuel or air gas flow in the i-stream. Twin premixed flames of the same fuel-air mixture in the lower and the upper stream are referred to as symmetric, while asymmetric denotes twin flames of unequal equivalence ratios.

1.2 Parabolic Profile at Nozzles Exit

The assumption of fully-developed parabolic flow field at the nozzles exit was first examined by [8,9]. The entrance length EL fig. 1. is the length of the tube necessary to have a fully developed parabolic profile. It is a function of many parameters, such as Reynolds number,

flow condition at the tube inlet, temperature gradients, tube surface, etc.
In the literature [10], an approximate value is assumed to be:

$$EL = \frac{L}{d} \cong 0.6\ Re \qquad \text{(Laminar flow)} \qquad (2)$$
$$EL = \frac{L}{d} \cong 4.4\ Re^{\frac{1}{6}} \qquad \text{(Turbulent flow)} \qquad (3)$$

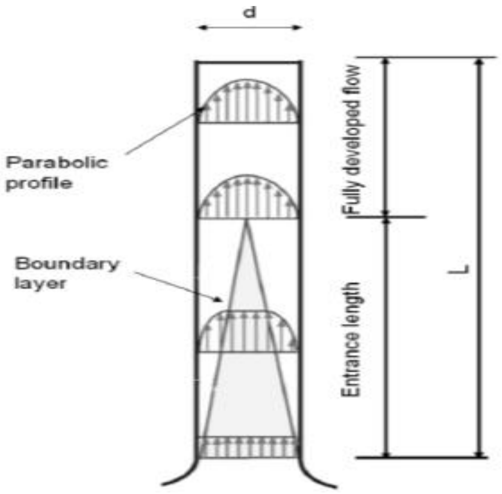

Fig. 1. Schematic of the entrance length in a tube [10].

1.3 Reaction Sheet Approximation

The mixture is introduced uniformly over the burner cross section at $Y = 0$ and $Y = L$, respectively. In the following, dimensional variables and unscaled mass fractions Y are designated by ~. It is assumed that both reactants follow Fick's law of mass diffusion and burn in a global one-step irreversible reaction [11]:

$$V_f\,\text{fuel} + V_x\,\text{oxidizer} \rightarrow \text{products} + Q \qquad (4)$$

Next, we make the drastic assumption of constant density $\bar{\rho}$ and transport properties (Di, K and Cp) independent of temperature. In addition, it is reasonable to assume that both reactants and the combustion products have identical $\overline{W}$, K, Cp, since both reactants are diluted with an inert (CO_2) that constitutes the bulk of the mixture.
As a consequence of $\bar{\rho} =$ constant, the bulk flow velocity $\tilde{U}$ becomes constant over the entire burner length. This simplifies the steady-state dimensional equations of conservation of species and energy to:

$$\tilde{\rho}\tilde{U}\frac{\partial \tilde{X}_0}{\partial \tilde{x}} - D_0\bar{\rho}\frac{\partial^2 \tilde{X}_0}{\partial\,\tilde{x}^2} = -V_0 W_0 \tilde{\omega} \qquad (5)$$
$$\tilde{\rho}\tilde{U}\frac{\partial \tilde{X}_f}{\partial \tilde{x}} - D_f\bar{\rho}\frac{\partial^2 \tilde{X}_f}{\partial\,\tilde{x}^2} = -V_f W_f \tilde{\omega} \qquad (6)$$
$$\tilde{\rho}Cp\,\bar{U}\frac{\partial \tilde{T}}{\partial \tilde{x}} - \lambda\frac{\partial^2 \tilde{T}}{\partial\,\tilde{x}^2} = \tilde{Q}\tilde{\omega} \qquad (7)$$

The system is made dimensionless, the reference temperature is $\frac{\tilde{q}}{Cp}$.
Where:

$$\tilde{q} = \frac{\tilde{Q}\tilde{X}_{F,L}}{V_f W_f} \qquad (8)$$

represents the heat released pure unit mass of fuel consumed.

1 EXPERIMENTAL SETUP

The counterflow apparatus consisted of two convergent nozzle burners with (12 mm) exit diameters vertically opposed brass tubes and were spaced (20 mm) apart. Outer thermal class box (20, 20, 20) cm, were used to isolate and stabilize the double flame in order to use three angles of nozzle (30, 45, 60 deg.) to compare the experimental data, fig. 2. gives the schematic of the counterflow nozzle burner. The improvement of data accuracy of measurement will be discussed later.

Consequently, the fuel (LPG) and oxidizer (air) streams respectively consisted of different equivalence ratio (0.65≤ ϕ ≤1.48). In addition, the mean exit velocities at the nozzles were kept equal.
The fuel was LPG of approximate composition (40% C_3H_8, 60 % C_4H_{10}), drawn from the mains by a compressor at a pressure of (1 bars) (gauge), and filtered to remove the dust particles, oil, and water droplets with diameters greater than 2μm.

Flow rates were metered by flowmeters calibrated by the manufactures and arranged, so that each burner could be supplied with (0-16 L/min) air and (0-6 L/min) of gas for premixed flames. The moment of the two jets was kept equal, so that the stagnation plane of the nonoscillating flow was located at the half distance, H/2, between the two opposing assemblies. Fig. 3. gives the schematic diagram of the experimental test rig, and the photo is shown in fig. 4.

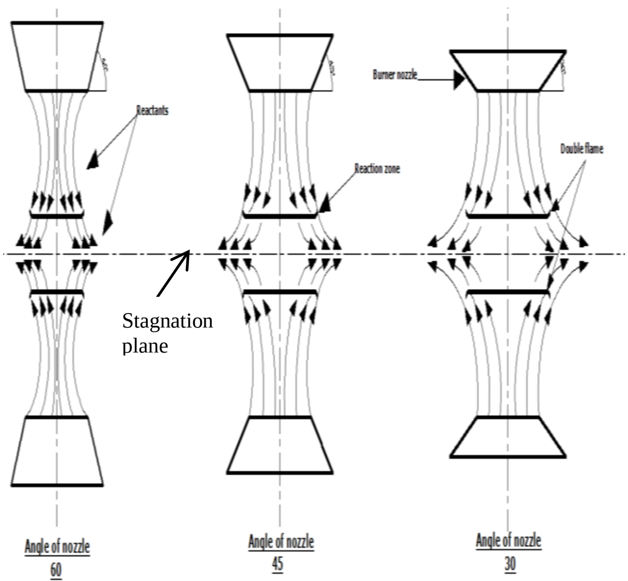

Fig. 2. Schematic illustration of the counterflow nozzle burner.

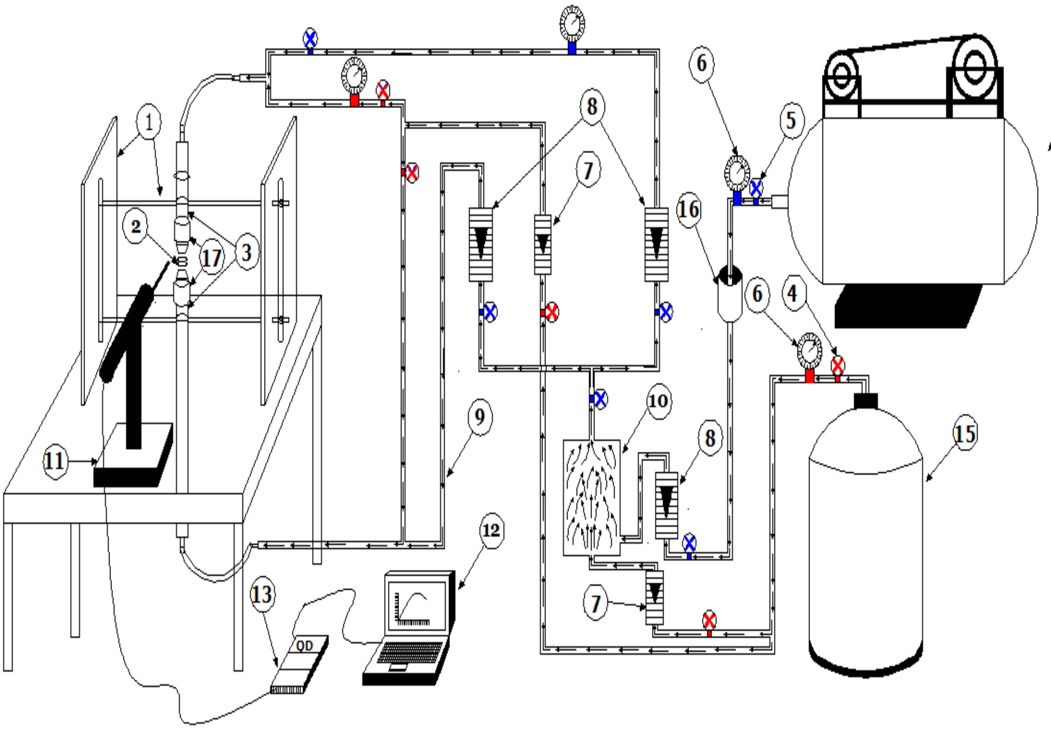

No.	name of parts
1	Burner holder
2	Double flame
3	Burners
4	Fuel valve
5	Air valve
6	Pressure gauge
7	Fuel flowmeter
8	Air flowmeter
9	Pipe
10	mixing chamber
11	Thermocouple Holder
12	Computer
13	QuickDAQ device
14	Compressor
15	Fuel cylinder
16	Air fillter
17	Water jacket

Fig. 3. Schematic diagram of the experimental test rig.

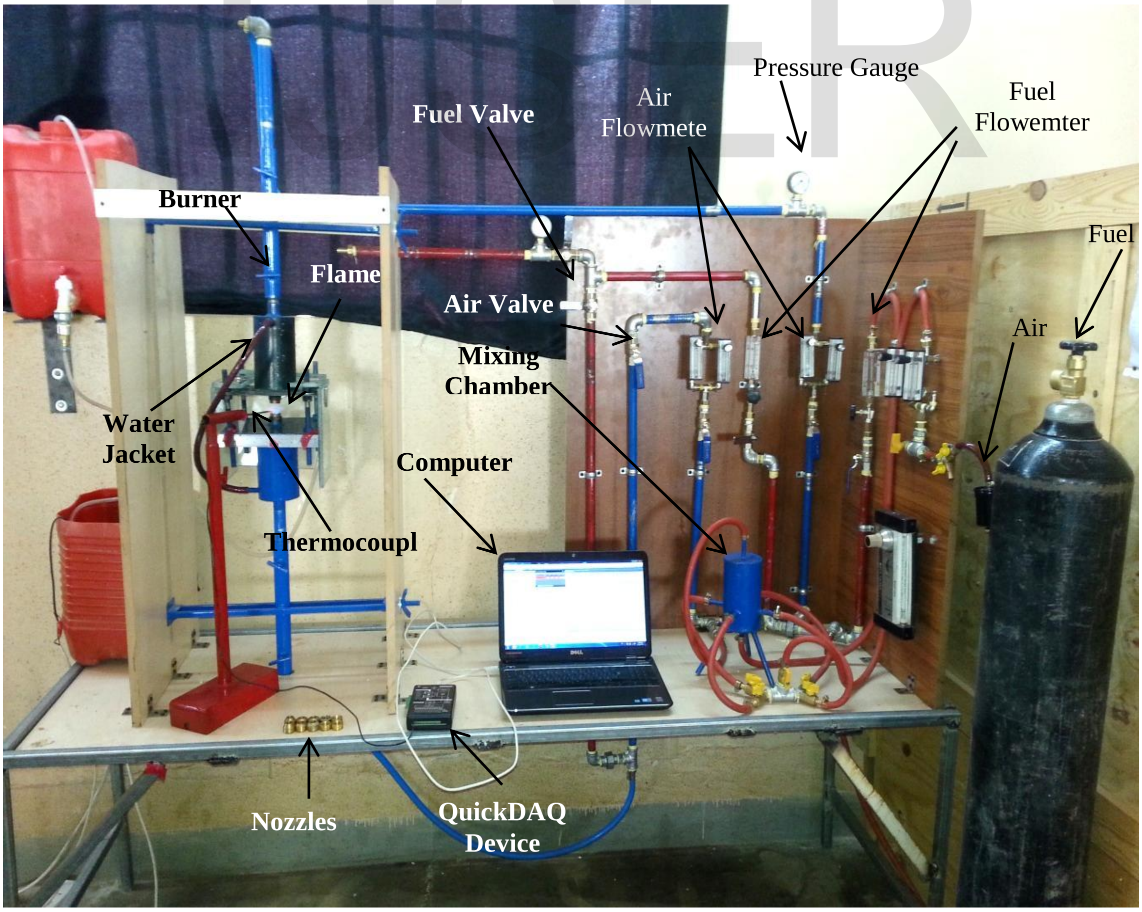

Fig. 4. Photograph of the counterflow burner facility.

2.1 Burner Characterization

Mixture composition profiles taken between the two injections were used to define the injection layer thickness, the effective boundary conditions and the mixture strength.

The contoured design of flow nozzle, coupled to (1/25)th cell size honeycombs, guarantees an exit velocity profile with reasonable uniformity. Contained several fine wire mesh screens near the nozzle exits, a standard technique causing the flow to be laminar [12, 13, 14].

The same burner can be used under diffusion and partially premixed conditions. In such a case, two identical premixed streams are fed to top and bottom burner, and twin flames are established symmetrically with respect to the gas stagnation plane.

The exit conditions were standard temperature and atmospheric pressure. The injection Reynolds number, based on the velocity of the mixture during the injection interval, the cold mixture viscosity and the exit nozzle diameter, was between $861.11 \leq Re_{jet} \leq 1377.78$, which corresponds to $1.105 \leq U_{jet} \leq 1.769$ m/s.

The burners were cooled using a closed loop water circulation at a fixed temperature between (28 and 35 °C) depending on the flame conditions and to avoid water condensation at the burner surfaces, fig. 5. shows the details of burners.

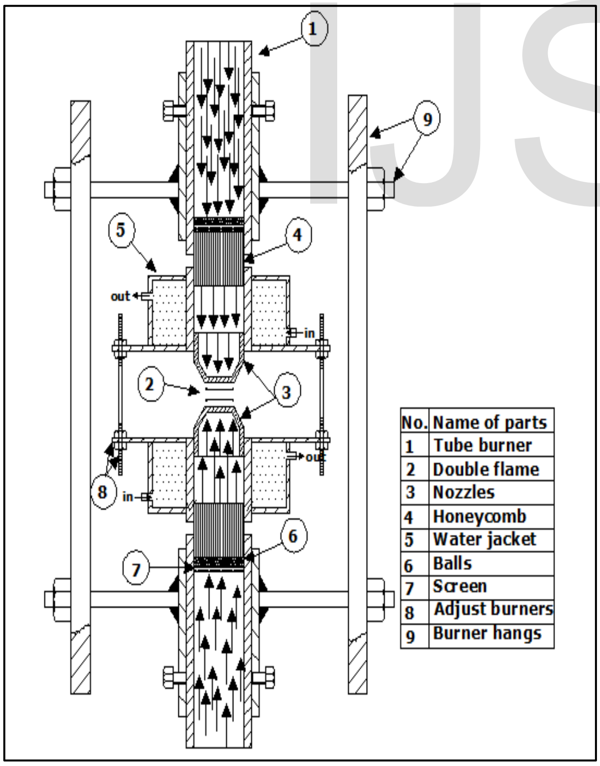

Fig. 5. details of burners.

3. RESULTS AND DISCUSSION

3.1 Flame Position

To measure the flame location in the burner, photographs were taken from the side. The images were then analyzed, and the flame position was determined as the point of maximum luminosity in the center between the burners. This optically determined flame location was checked to be in excellent agreement with the location of temperature maximum. The flames were stabilized about the point where the mean velocity of propagation equals the mean axial flow velocity of the reactants. The flame surfaces appeared undulatory and rapidly changing about this stable mean position. The effects of buoyancy were more pronounced in making the flow asymmetric at lower flow velocities and large nozzle separation.

3.2 Limits of Operation

The discussion concerning flame stability is also aided considerably the use of a combustion diagram, as long as the fuel-air mixture is combustible. There are four limits of operation of the reacting counterflowing: jets blow-off, double flame, disc flame, and distortion flame, as shown in fig. 6., as a function of the air and fuel flow rate from the nozzle exit, their photos are shown in fig. 7.

The concept of flame lift can be attributed to the stream velocity through the flame parts not being balanced by burning velocity of the fuel-air mixture. If the primary aeration rises, both the burning velocity and the volume flow through the flame ports increase. However, the latter increases more than the former, and thus flame lift may occur. If the velocity is further increased, a point will be reached at which the flames will be extinguished.

The double-disc flame can be obtained when the velocity of air and fuel mixture equal to the burning velocity, which leads to the separator between the surfaces of the discs called stagnation plane. At the same area, but installing the fuel velocity constant and increase the air velocity, the discs come together and be a single disc, because the velocity of the mixture is greater than the velocity of the reactants which the reactants occur in one area, as shown in Fig. 6.

Either install the air velocity or increase the velocity of fuel leads clearly to a flame distortion, and the appearance of soot and carbon monoxide is in the yellow flame zone.

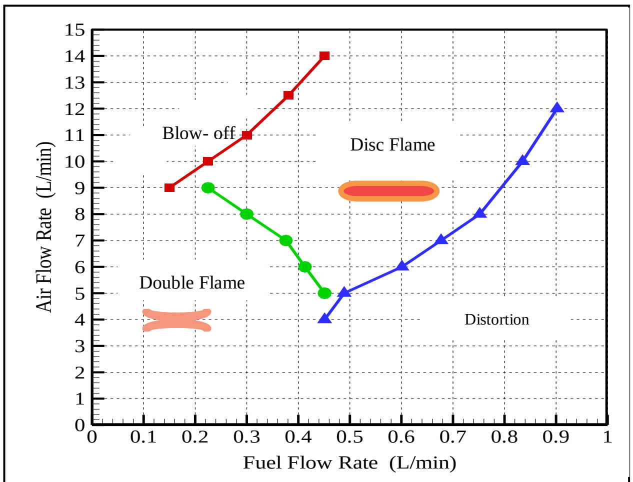

Fig. 6. Stability limits of flame in counterflow

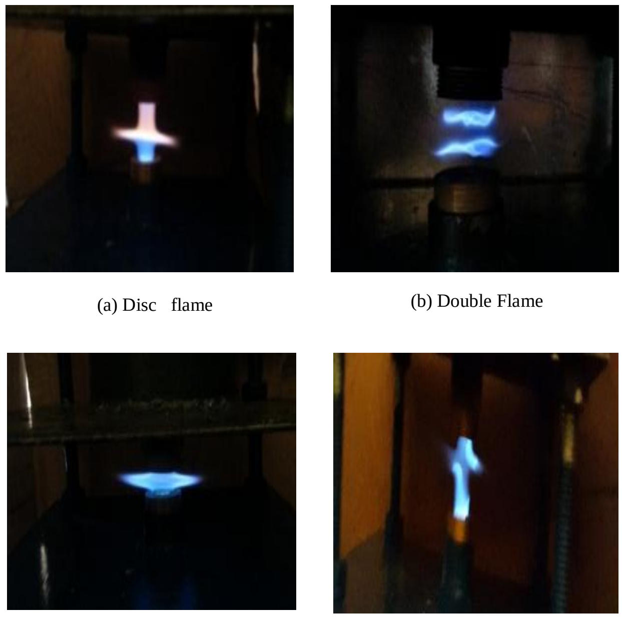

(a) Disc flame (b) Double Flame

(c) Disc Flame (d) Distortion Flame

Fig. 7. Photo of types of counterflow flame

3.3 Burning Velocity

The design of the combustion chambers and industrial furnaces depends on the shape of the temperature distribution, the diameter of flame front and burning velocity.

A wide range of equivalence ratios has been used in different experiments, from fuel lean mixtures to fuel rich mixtures ($0.65 \leq \phi \leq 1.48$). This ratio directly affects the sooting tendency and level of dissociation in the combustion product. The flames at nearly stoichiometric conditions produce the highest burning velocity due to complete combustion. Fuel rich flames ($\phi > 1$) produce both luminous and non-luminous thermal radiation, where the flames near stoichiometric condition ($\phi = 1$) produce only non-luminous radiation, since no soot is generated.

The burning velocity was measured to three nozzles at different angles (30°, 45°, and 60°) and different distances between the nozzles burners (H = 20, 30, and 40 mm). Through figs. 8, 9, and 10. it was noted that the burning velocity depends on the stagnation surface of the flame front, which in turn relies on the vertical distance between the burners (H). Also, it was noticed that the increase in distance between the burners leads to a decrease in the velocity of the reactants since it is affected by the air surrounding, that leading to the outside air participate in the interaction and thus affected on the equivalence ratio of the chemical mixture and reduced the burning velocity.

Additionally, it was observed through figs. 8, 9, and 10. there was an increase in the deflection jet angle with the horizontal axis that leads to the faster of the reactants and reduces the vortices near the burner nozzle rim, due to decrease of friction force between the tube wall jet and reactant molecules. And, at the same time, it helps to the faster exit of reactants toward the stagnation surface and flame front consists.

Where the area of disc flame changes with the jet angle for the same equivalent ratio, according to the following results at the nozzle angles (30°- Df = 56 mm), (45° - Df = 53 mm), and (60° - Df = 50 mm). Comparing the results obtained with previous studies, it was noted that there is a consensus between them with an increase in the burning velocity of a jet (60°), especially at the equivalence ratio ($\phi = 1$), fig. 11. shows the results obtained in the current research compared with previous studies.

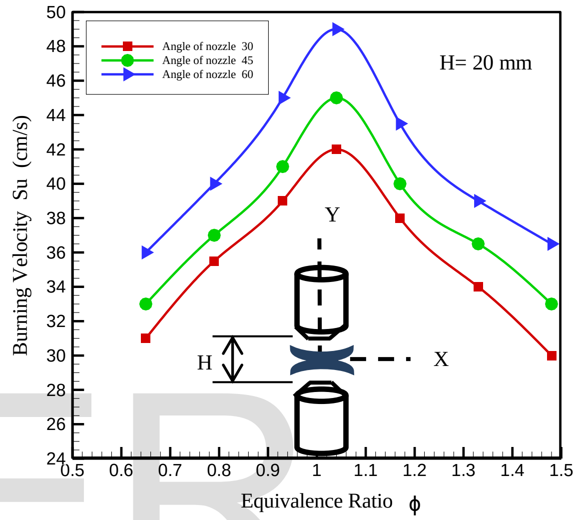

Fig. 8. Effect types of nozzle on burning velocity at (H= 20mm).

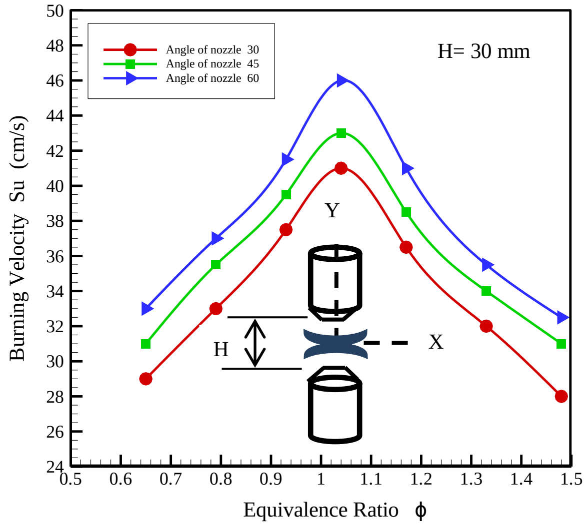

Fig. 9. Effect types of nozzle on burning velocity at (H= 30mm).

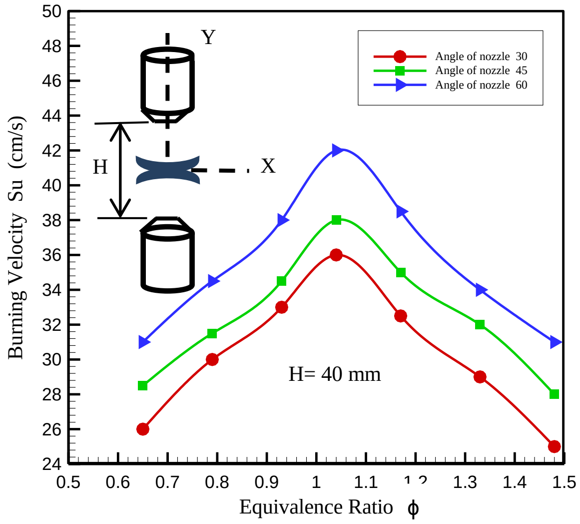

Fig. 10. Effect types of nozzle on burning velocity at (H= 40mm).

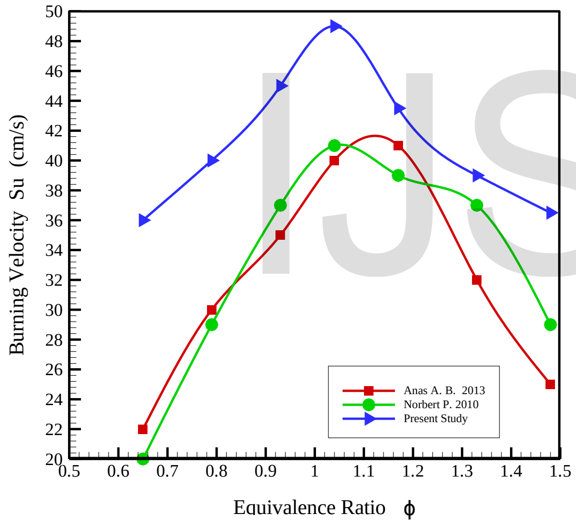

Fig. 11. Compare burning velocity with previous study.

4. CONCLUSIONS

Based on a limited amount of experimentation, several conclusions can be made regarding the use of laminar counterflowing jets for combustion research.

1- Flame front disc in counterflow burner depends on the burner design and location of honeycomb, screen and bolls.
2- Limits of stability in the counterflow (blow-off flame, double flame, disc flame, and distortion flame) depend basically on the shape of the jet and velocity of fuel and air.
3- The higher vertical distance (H) between the burners led to a decrease in the burning velocity since it was affected by the external surroundings.
4- Diameter of disc flame front in the counterflow burner increases with the nozzle angle decrease.
5- Increasing the jet angle increases the burning velocity, because a few effects of the reactants with the surface of the jet decrease the vortices.
6- Burning velocity depends on the stoichiometric ratio, where the greatest value is noted when the ratio ($\phi = 1$) and begins to decrease from both sides rich and lean.

ACKNOWLEDGMENTS

The author would like to thank and acknowledge the staff of workshop in Sulaimani Polytechnic University-Engineering Technical Collage for helping to construct the test rig.

NOMENCLATURE

AR	Air flow rate	$L.min^{-1}$
FR	Fuel flow rate	$L.min^{-1}$
A/F)a	Actual air to fuel ratio	-
A/F)st	Stoichiometric air to fuel ratio	-
Cp	Specific heat at constant pressure	$kJ.kg^{-1}.k^{-1}$
d	Internal tube diameter	mm
Df	Flame diameter	mm
Di	Diffusivity of species I	$m^2.\ s^{-1}$
EL	Entrance length	-
L	Tube length	mm
LPG	Liquefied petroleum gas	-
Q	Total heat released	$kJ.s^{-1}$
$\dot{\emptyset}$ fuel	Fuel volume flow rate	$L.min^{-1}$
$\dot{\emptyset}$ air	Air volume flow rate	$L.min^{-1}$
q	Heat released per unit mass of fuel	$kJ.s^{-1}$
Re	Reynolds number	-
T	Flame temperature	K
$\tilde{U}$	Bulk flow velocity	$m.s^{-1}$
Wi	Molecular weight of specie I	$Kmol.m^{-3}$
X	Axial distance	mm
XF	Fuel mass fraction	-
XO	Oxidizer mass fraction	-
Y	Vertical distance	mm

Greek Symbols

λ	thermal conductivity of mixture	$W.m^{-1}.K^{-1}$
υ_i	Stoichiometric coefficient of species I	-
ρ	Density	$Kg\ .\ m^{-3}$
Φ	Equivalence ratio	-
Φi	Equivalence ratio of the ith stream	-
ω	Chemical reaction rate	$Mol.s^{-1}$

REFERNCES

[1] Chelliah, H. K., and Williams, F. A.,Twenty-Third Symposium (International) on Combustion, the combustion Institute, Pittsburg, p. 503, 1990.

[2] Mounaim, C., and Gokalp, I., "Spring meeting of the Western States of the Combustion Institute, Salt Lake City, Utah, 1993.

[3] Katerina, A. M., and Whitelaw, J. H."Extinction of turbulent counterflow flames under periodic strain", Combustion and Flame, 120: 265-284 (2000).

[4] Matynia, A., Pillier, M., Delfau, J., Chauveau, C., and Vovelle, Centre National de Recherche Scientifique ICARE-Institute de Combustion, Proceeding of the European Combustion, 2009.

[5] Bray, K. N., Libby, P. A., and Moss, J. B., "Flamelet crossing frequencies and mean reaction rates in premixed turbulent combustion", Combustion Science and Technology, 41: 143, 1984.

[6] Gouldin, F. C., "An application of fractals to modeling premixed turbulent flames" Combustion and Flame, 68: 249, 1987.

[7] Kostiuk, L. W., Bray, K. N., and Chew, T. C. "Premixed Turbulent Combustion in Counterflowing Streams", Combustion Science and Technology, 64: 233-241, 1989.

[8] Frozakis, C. E., Tomboulides, A. G., Lee, J., and Boulouchos, K., "Diffusion to Premixed flames in an H2/air opposed-jet burner". Combustion and Flame, 130: 171-184, 2002.

[9] Frozakis, C. E., Tomboulides, A. G., Lee, J., and Boulouchos, K., "Transient phenomena during diffusion/ edge flame transitions in an opposed-jet hydrogen/air burner", Proceeding of the Combustion Institute, 29: 1581-1587, 2003.

[10] Andrea, C., "Hydrogen and methane edge and diffusion flames in opposed jet configurations", for the Ph.D. Thesis of technical sciences, Swiss Federal Institute of Technology Zurich, 2006.

[11] Robert, E., and Monkewitz, P. A., " Experiments in a novel quasi-ID diffusion flame with variable bulk flow" Proceeding of the Combustion Institute, 32: 987-994, 2009.

[12] Hamins, A., Thridandam, H., and Seshadri, K., Chemical Engineering Science, 40: 2027-2038, 1985.

[13] Puri, I. K., "The structure and extinction of counterflow flames", Ph.D. Thesis, University of California, San Diego. 1987.

[14] Yong, L., Don, J., and Ishwar, K., "Heat release mechanisms in inhibited laminar counterflow flames", Fire, Combustion and Hazardous Waste Processing, ASME vol. 296, 1994.

[15] Anas, A. B., "Determination of laminar burning velocities" master's thesis, Lunds University, 2013. [16] Norbert, P. "Combustion Theory", Rwth. Aachen University, 1st edition books, 2010.